Synthesis and characterization of chromium doped boehmite nanofibres

Jing (Jeanne) Yang, [1] Ray L. Frost [1•] and Yong Yuan [1,2]

[1] Inorganic Materials Research Program, School of Physical and Chemical Sciences, Queensland University of Technology, GPO Box 2434, Brisbane Queensland 4001, Australia.

[2] Institute of Solid State Physics, Chinese Academy of Sciences, Hefei 230031, China.

Abstract

Thermogravimetric and differential thermogravimetric analysis has been used to study synthesised chromium doped boehmite. The dehydroxylation temperature increases significantly from 0% to 5% doping, after which the dehydroxylation temperature shows a small steady increase up to the 20% doping level. The temperature of dehydroxylation increases with time of hydrothermal treatment. Chromium doped boehmite nanofibres were also characterised by X-ray diffraction and transmission electron microscopy. Hydrothermal treatment of doped boehmite with chromium resulted in the formation of nanofibres over a wide dopant range. Nanofibres up to 500 nm in length and between 4-6 nm wide were produced.

Key words: boehmite, chromium doping, nanofibres, nanomaterial, transmission electron microscopy, thermal analysis, thermogravimetry

• Author to whom correspondence should be addressed (r.frost@qut.edu.au)

Introduction

Compared to their micro and macro counterparts, nanosized materials have been received wider attention because of their intrinsic properties, which are determined by their composition, size, shape, and structure. [1] Such as nanofibers, nanotubes, nanoribbons and nanorods, one dimensional (1D) nanoscale inorganic materials have attracted intensive interest due to their distinctive geometries, novel physical and chemical properties, and the potential applications in many fields. [2] Boehmite (γ -AlOOH) and its oxide derivatives such as α-Al_2O_3 and γ -Al_2O_3 have been studied extensively because they can be used as catalysts, adsorbents, flame retardants and optical materials. [3-6]

Synthesis forms an essential component of nanoscience and nanotechnology. While nanomaterials have been generated by physical methods such as laser ablation, arc-discharge and evaporation, chemical methods have proved to be more effective, as they provide better control as well as enable different sizes, shapes and functionalization. Among these methods, hydrolysis and precipitation are the most common. John Bugosh first synthesized the boehmite nanofibers by a hydrothermal method in 1961. [7] Since then, numerous studies on boehmite nanofibers have been undertaken, for example, boehmite (AlOOH) nanofibers were reported to be assembled with the assistance of poly(ethylene oxide) (PEO) surfactant [8] and tubular γ -Al_2O_3 was fabricated via soft solution route using *N*-cetyl-*N*,*N*,*N*-trimethylammonium bromide (CTAB) surfactant. [9] Shen et al. published a report showing a steam-assisted solid-phase conversion of amorphous aluminium hydroxides wet gel to well crystallized 1D nanostructure of boehmite AlOOH nanorods without using surfactants and solvents. [10] The process is unique in the simplicity of preparation and the high efficiency of crystal growth, which can be operated at a large scale.

As for doping clays, the addition of other metal ions into boehmite, especially into nanostructured boehmite would have great potential to contribute the further application of these inorganic nanomaterials due to the enhancement of its properties, and there have been reports on boehmite doped by Fe, Ga and Eu. [11-13] It is also reported that materials doped with chromium could obtain special electric, magnetic

or optical properties and gain more application. [14-17] This paper reports our research on Cr-doped boehmite. Such concepts have not been previously reported.

Thermal analysis has been proved as the most useful method for the analysis of minerals and related materials. In this work, boehmite nanofibers based on Shen's methodology [10] were synthesised by introducing chromium as dopant and a series of chromium doped boehmite nanofibers with different chromium content percentage and varying hydrothermal treatment time have been systematically studied with the thermo gravimetric techniques.

Experimental

Synthesis of chromium doped boehmite nanofibers

A total amount of 0.02 moles of aluminium nitrate and chromium nitrate were mixed before being dissolved in ultra-pure water. To make a comparison, mixtures with chromium molar percentage of 0, 1, 3, 5, 10 and 20 % were prepared separately and then dissolved in ultra-pure water to form solutions with a metal ion to H_2O molar ratio of 1:35. At room temperature, 10% by weight ammonia solution was added dropwise into the metal ions solution while stirring vigorously. The addition of the ammonia solution was ceased when the pH value of the reaction mixture reached 5. The mixture was then stirred at room temperature for 1 hour. The obtained gel was filtrated to obtain the wet gel-cake, which was then transferred into a 25mL glass beaker. Before putting the beaker with gel-cake into a Teflon vessel (125mL), 2ml ultrapure water was poured to the bottom of each vessel separately. The Teflon vessels were sealed and heated them at 170ºC for 1, 3, 5 and 10 days. The resulting materials were washed several times with ultrapure water, centrifuged, and dried in air at 35ºC for 2 days.

X-ray diffraction

XRD analyses were performed on a PANalytical X'Pert PRO X-ray diffractometer (radius: 240.0mm). Incident X-ray radiation was produced from a line focused PW3373/10 Cu X-ray tube, operating at 40kV and 40mA, wavelength of 1.54Å.

TEM analysis

A Philips CM 200 transmission electron microscopy (TEM) at 200 kV was used to investigate the morphology of the boehmite nanofibers. All samples were dispersed in absolute ethanol solution and then dropped on copper grids.

Thermal analysis

Thermal decomposition of the Cr-doped boehmite was carried out in a TA® Instrument incorporating a high-resolution thermo gravimetric analyser (series Q500) in a flowing nitrogen atmosphere ($60cm^3\ min^{-1}$). Approximately 20mg of each sample underwent thermal analysis, with a heating rate of 5°C/min, with resolution of 6 from 25 to 1000°C. With the isothermal, isobaric heating program of the instrument the furnace temperature was regulated precisely to provide a uniform rate of decomposition in the main decomposition stage.

Results and discussion

X-ray diffraction

X-ray diffraction was normally used to determine the phase and purity of the synthesized materials. Figure 1a and 1b display well-defined XRD patterns observed and all diffraction peaks were perfectly indexed to the XRD pattern of undoped boehmite (JCPDS card 01-083-2384). No XRD peaks representing other crystalline phases were detected, indicating that the chromium doped nanofibers of the synthetic boehmite exhibited excellent crystallinity and a high purity. Figure 1a shows that the peaks are higher and narrower with the increase of the hydrothermal treatment time to 10 days, which means the crystals grew better as synthesis time getting longer.

Transmission electron microscopy

The transmission electron microscopy images of the synthesised undoped and Cr-doped boehmite are shown in Figures 2. The figures show the TEM images of (a) undoped boehmite, (b) 3% Cr-doped and (c) 5% Cr-doped. The figures clearly show that the boehmite is fibrous with very long narrow fibres often exceeding 500nm in

length and with widths of between 2 and 6nm. Many of the fibres are curved or bent as may be observed in Figure 2c for the 5% Cr-doped boehmite.

Thermogravimetric analysis

The thermogravimetric analysis and the differential thermal analysis of nanostructured undoped boehmite and doped boehmite with varying amounts of chromium dopant from 0 to 20% are shown. The thermal analysis pattern of undoped boehmite is displayed in Figure 3a. Figures 3b to e report the effect of hydrothermal treatment time on the formation of boehmite nanofibres. Figure 4 shows the effect of the % of doping on the thermal analysis of Cr doped boehmite. The results of the thermal analyses are summarised in Table 1.

The TG of the undoped boehmite shows a strongly asymmetric curve with a peak temperature of 406.5°C and a mass loss of 15.8%. The thermal decomposition occurs as follows: $2AlO(OH) \rightarrow Al_2O_3 + H_2O$. This major decomposition step is attributed to the dehydroxylation of the boehmite**.** Two low mass loss steps at 45 and 260°C with mass losses of 1.5 and 1.7% are also observed. The first mass loss step is assigned to the dehydration of boehmite (Column 1 in Table 1)

The thermal decomposition of 1% doped boehmite with 1 day hydrothermal treatment shows three mass loss steps at 46, 311 and 403°C with mass losses of 1.7, 6.6 and 11.0% (Figure3b). The asymmetry observed in Figure 3a is no longer observed but a second peak at 311°C is found. The thermal decomposition of 1% doped boehmite with 3 day hydrothermal treatment shows three mass loss steps at 50, 321 and 419.5°C with mass losses of 1.0, 4.8 and 11.5% (Figure 3c). The thermal decomposition of 1% doped boehmite with 5 day hydrothermal treatment shows three mass loss steps at 51, 328 and 423°C with mass losses of 0.8, 3.9 and 12.1% (Figure 3d). The results of the 1% Cr doped boehmite hydrothermally treated for 10 days (Figure 3e) shows a large mass loss step at 435°C with a mass loss of 12.2%. In addition two smaller mass loss steps at 54 and 342°C with mass losses of 0.7 and 3.1% are observed. It is apparent that thermal decomposition temperature of the Cr doped

boehmite varies with the hydrothermal treatment time. This variation is reported in Figure 5.

The variation in the % chromium doping on the thermal analysis patterns and decomposition of boehmite is explored in Figures 4a to 4d. The thermal analysis patterns of 3% Cr doped boehmite hydrothermally treatment for 3 days shows three mass loss steps at 46, 315 and 427°C with mass losses of 1.1, 2.9, and 12.4%. The dehydroxylation peak at 427°C is sharp indicating that the dehydroxylation occurs over a very narrow temperature range. For the 5% Cr doped boehmite the dehydroxylation step is observed at 430.5°C with a mass loss of 13.1%. For the 10% Cr doped boehmite hydrothermally treated for 3 days results in a sharp mass loss peak at 433°C with minor mass loss steps at 50 and 380°C. The temperature for the Cr 20% doped boehmite is 436.5°C. The variation in the temperature of the decomposition of boehmite as a function of % doping is reported in Figure 6. It is apparent that as the % of Cr is increased in the boehmite the dehydroxylation temperature is increased and shifts from 406.5°C to 436.5°C.

The variation of the dehydroxylation temperature and associated mass loss with the % of Cr doping is shown in Figure 6. As the dehydroxylation temperature increases the mass loss from the dehydroxylation step decreases. The dehydroxylation temperature increases significantly from 0% to 5% doping, after which the dehydroxylation temperature shows a small steady increase up to the 20% doping level. The associated mass loss decreases and then shows a constant mass loss. The variation of mass loss and dehydroxylation temperature with hydrothermal treatment time is illustrated in Figure 7. The temperature of dehydroxylation increases with time of hydrothermal treatment.

Conclusions

Boehmite and chromium doped boehmite were synthesized by low temperature precipitation from aqueous solution and hydrothermally treated for differing time intervals. Very long nanofibres were produced often exceeding 500nm in length. Normally at above the 5% doping level a mixture of nanofibres are produced.

Doping with chromium resulted in an increase in the dehydroxylation temperature of boehmite from ~406.5°C to 436.5°C. The temperature of dehydroxylation increases with time of hydrothermal treatment. The dehydroxylation temperature increases significantly from 0% to 5% doping, after which the dehydroxylation temperature shows a small steady increase up to the 20% doping level.

Acknowledgements

The financial and infra-structure support of the Queensland University of Technology Inorganic Materials Research Program of the School of Physical and Chemical Sciences is gratefully acknowledged. The Australian Research Council (ARC) is thanked for funding the instrumentation.

References

[1] Y.G. Sun, Y.N. Xia, Science 298 (2002) 2176-2179.

[2] M.S. Gudiksen, L.J. Lauhon, J. Wang, D.C. Smith, C.M. Lieber, Nature 415 (2002) 617-620.

[3] D. Mishra, S. Anand, R.K. Panda, R.P. Das, Materials Letters 42 (2000) 38-45.

[4] V.S. Burkat, V.S. Dudorova, V.S. Smola, T.S. Chagina, Light Metals (Warrendale, PA, United States) (1985) 1443-1448.

[5] J.-L. Le Loarer, H. Nussbaum, D. Bortzmeyer, Alumina extrudates, methods for preparing and use as catalysts or catalyst supports. (Rhodia Chimie, Fr.). Application: WO, 1998, p. 44.

[6] C. Nedez, J.-P. Boitiaux, C.J. Cameron, B. Didillon, Langmuir 12 (1996) 3927-3931.

[7] J. Bugosh, Journal of Physical Chemistry 65 (1961) 1789-1792.

[8] H.Y. Zhu, X. P.Gao, D. Y. Song, Y. Q. Bai, S. P. Ringer, Z. Gao, Y. X. Xi, W. Martens, J. D. Riches, R.L. Frost., J. Phys. Chem. B 108 (2004) 4245-4247.

[9] D. Kuang, Y. Fang, H. Liu, C. Frommen, D. Fenske, Journal of Materials Chemistry 13 (2003) 660-662.

[10] S.C. Shen, Q. Chen, P.S. Chow, G.H. Tan, X.T. Zeng, Z. Wang, R.B.H. Tan, J. Phys. Chem. C 111 (2007) 700-707.

[11] Y.Y. Zhao, W.N. Martens, T.E. Bostrom, H.Y. Zhu, R.L. Frost, Langmuir 23 (2007) 2110-2116.

[12] Y.Y. Zhao, R.L. Frost, W.N. Martens, Journal of Physical Chemistry C 111 (2007) 5313-5324.

[13] J.M.A. Caiut, S.J.L. Ribeiro, Y. Messaddeq, J. Dexpert-Ghys, M. Verelst, H. Dexpert, Nanotechnology 18 (2007).

[14] K. Fujita, Y. Tokudome, K. Nakanishi, K. Miura, K. Hirao, Journal of Non-Crystalline Solids 354 (2008) 659-664.

[15] Y.C. Huang, J.S. Wang, Y.K. Lu, W.K. Liu, K.Y. Huang, S.L. Huang, W.H. Cheng, Optics Express 15 (2007) 14382-14388.

[16] C.G. Jin, X.M. Wu, L.J. Zhuge, Z.D. Sha, B. Hong, Journal of Physics D-Applied Physics 41 (2008).

[17] S.M. Abo-Naf, M.S. El-Amiry, A.A. Abdel-Khalek, Optical Materials 30

Table 1

Sample	Decomposition steps			Peaks			total mass loss (%)
	Step 1	Step 2	Step 3	Peak 1	Peak 2	Peak 3	
boehmite	1.5%	1.7%	15.8%	45°C	260°C	406.5°C	19.0%
1% - 1d	1.7%	6.6%	11.0%	46°C	311°C	403°C	19.3%
1% - 3d	1.0%	4.8%	11.5%	50°C	321°C	419.5°C	17.3%
1% - 5d	0.8%	3.9%	12.1%	51°C	328°C	423°C	16.8%
1% - 10d	0.7%	3.1%	12.2%	54°C	342°C	435°C	16.0%
3% - 3d	1.1%	2.9%	12.4%	46°C	315°C	427°C	16.4%
5% - 3d	0.8%	2.1%	13.1%	48°C	325°C	430.5°C	16.0%
10% - 3d	0.8%	-	15.1%	50°C	380°C	433°C	15.9%
20% - 3d	1.0%	-	15.0%	50°C	330°C	436.5°C	16.0%

* "d" means "days of hydrothermal treatment"

LIST OF FIGURES

List of Tables

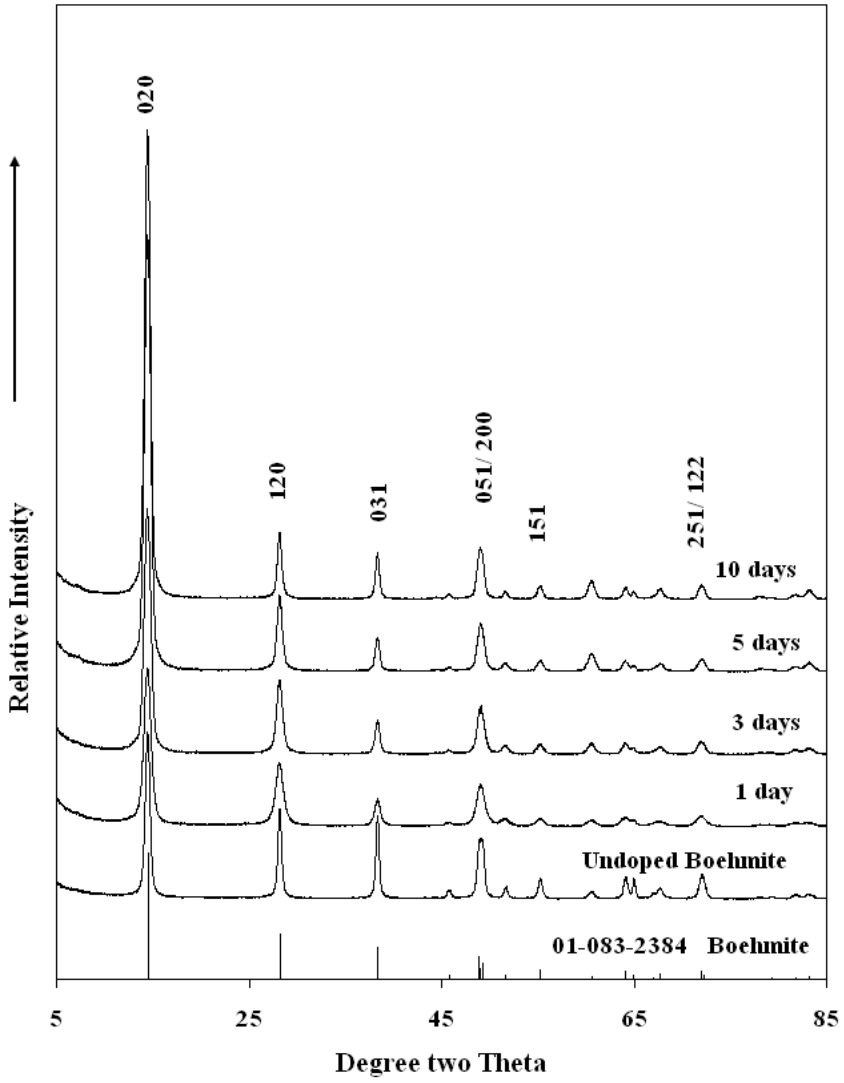
020
120
031
051/ 200
151
251/ 122
10 days
5 days
3 days
1 day
Undoped Boehmite
01-083-2384 Boehmite
Relative Intensity
5
25
45
65
85
Degree two Theta

Figure 1a

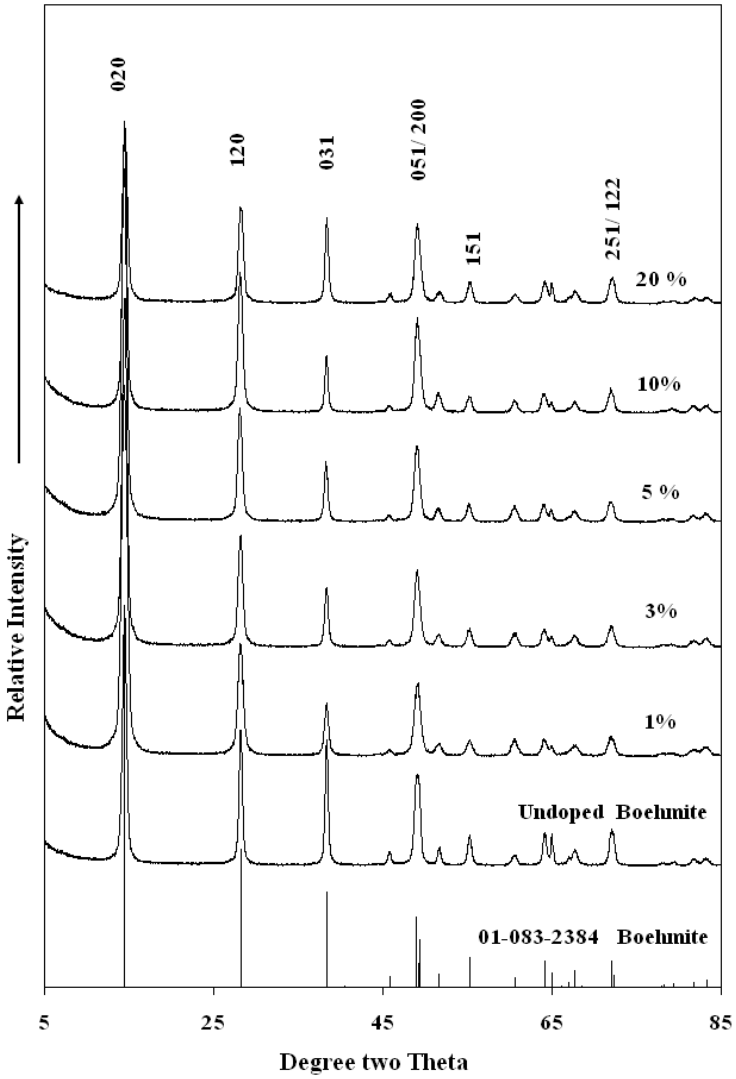

296

297

298 **Figure 1b**

299

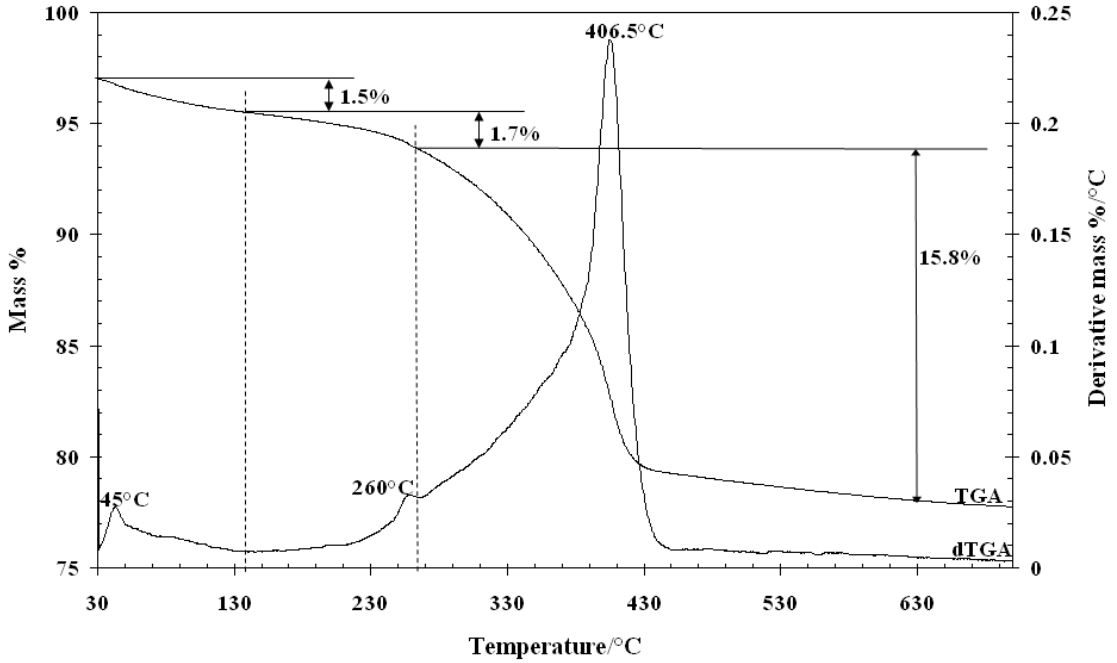

Figure 3(a) undoped boehmite

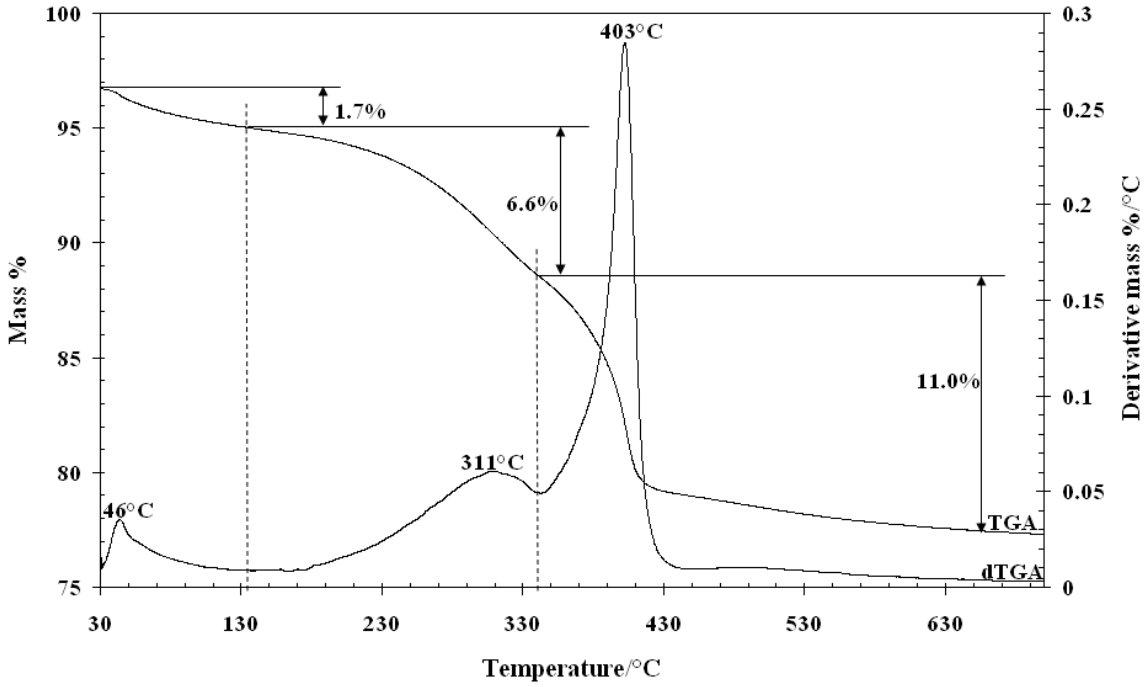

Figure 3(b) 1 day 1%Cr-doped

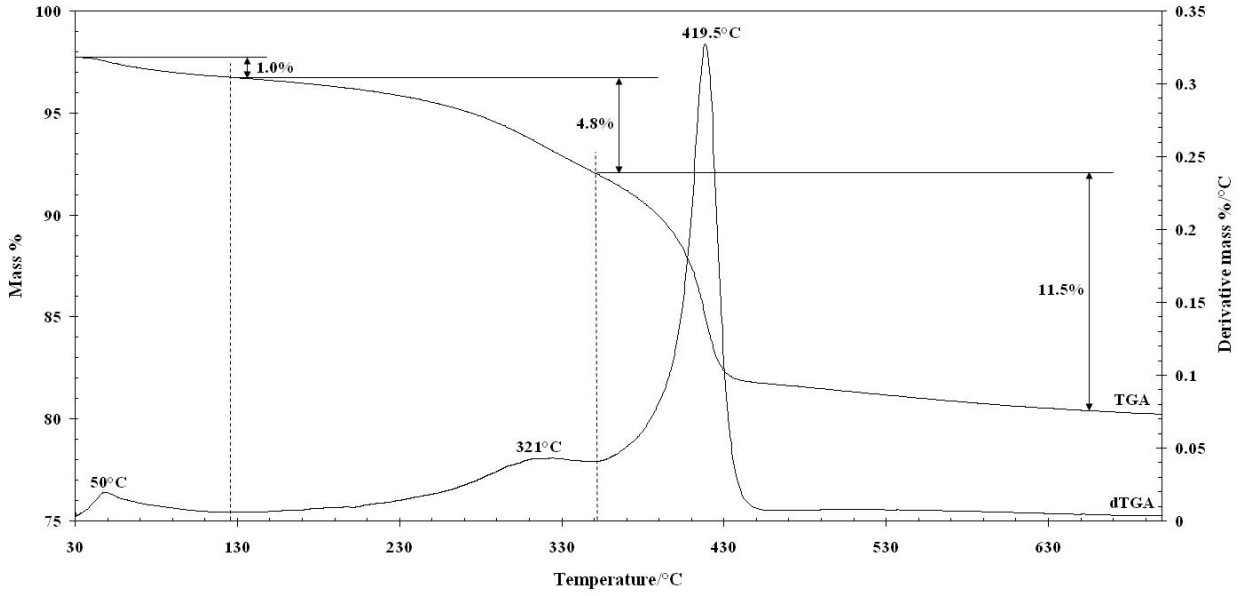

Figure 3(c) 3 days 1%Cr-doped

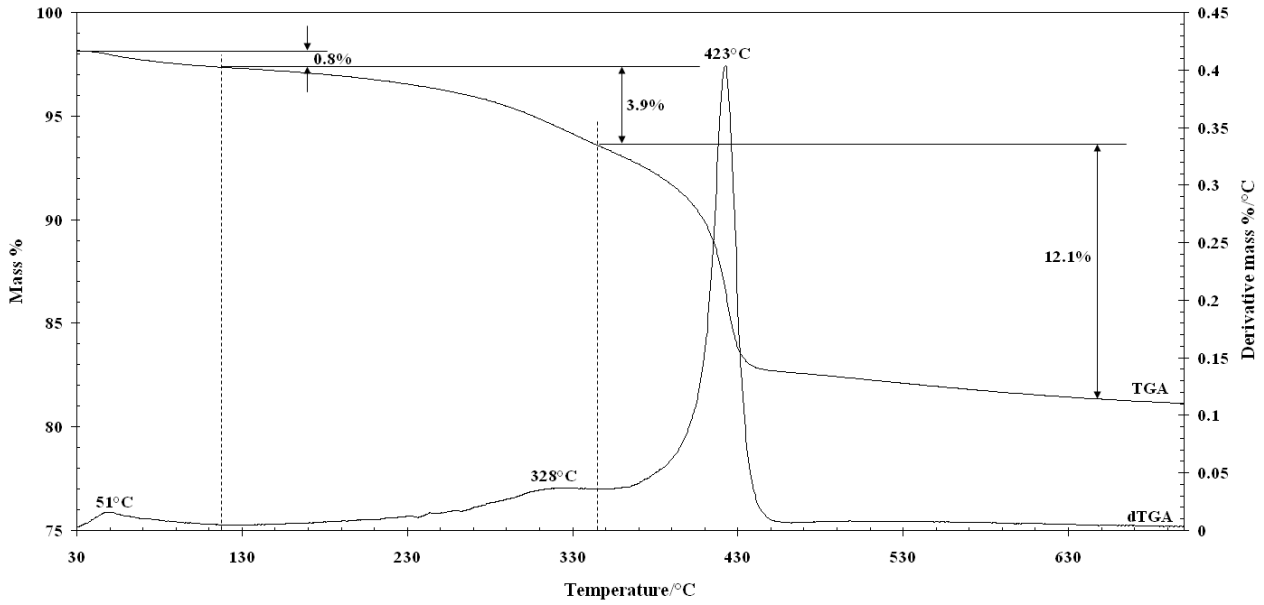

Figure 3(d) 5 days 1%Cr-doped

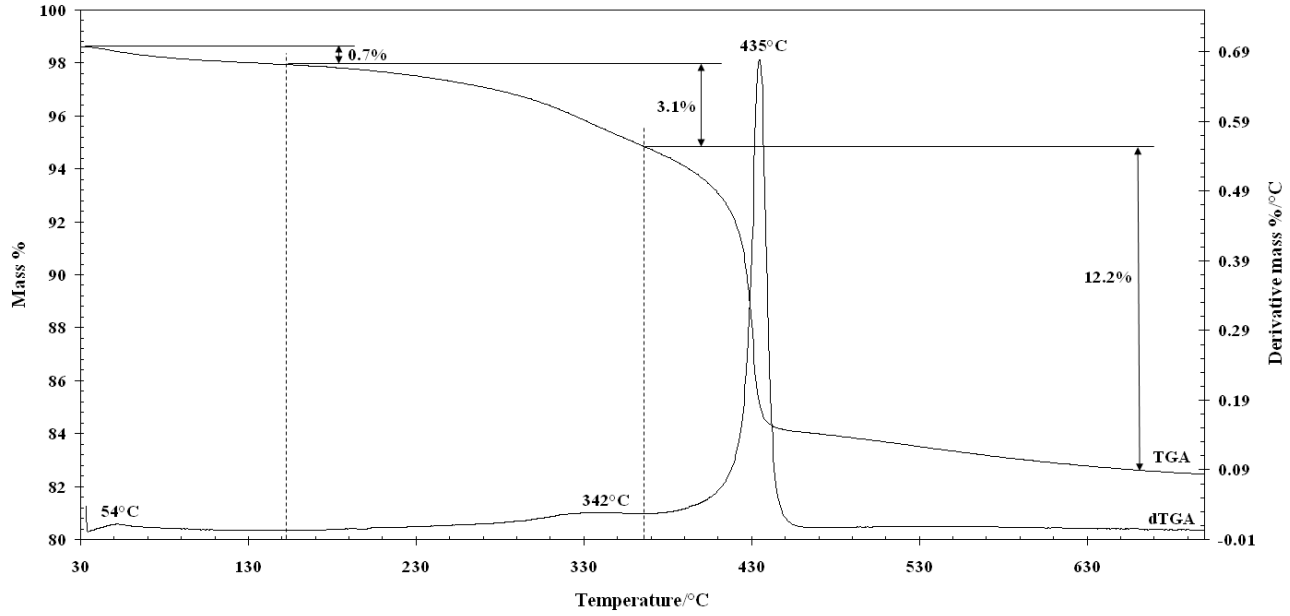

Figure 3(e) 10 days 1%Cr-doped

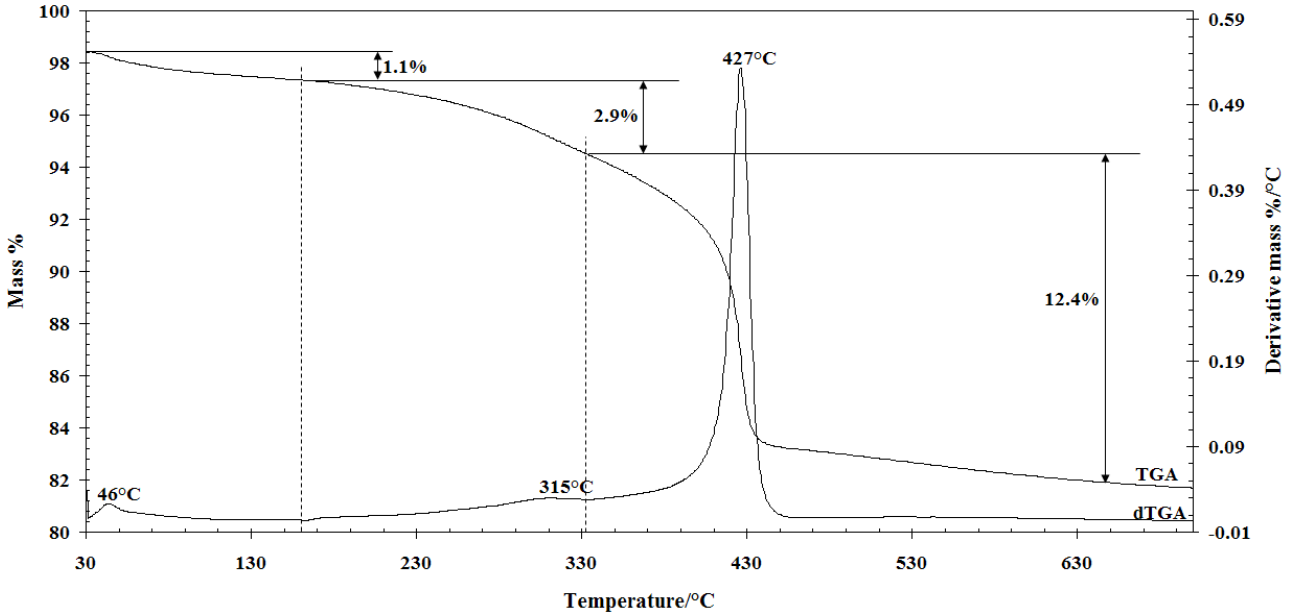

Figure 4(a) 3 days 3% Cr-doped

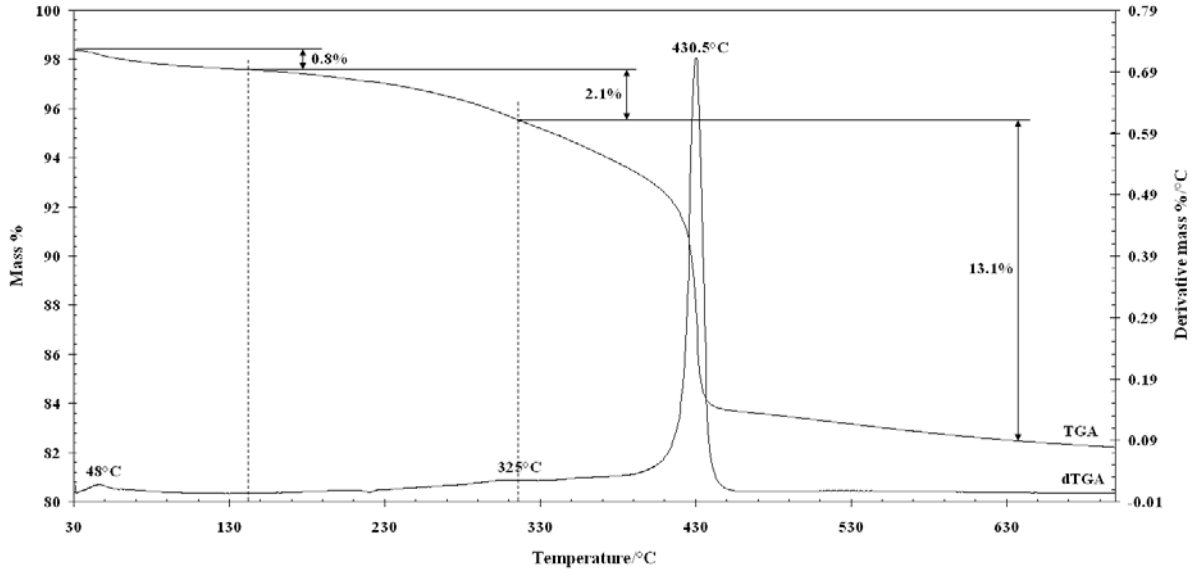

362

363 **Figure 4(b) 3 day 5% Cr-doped**

364

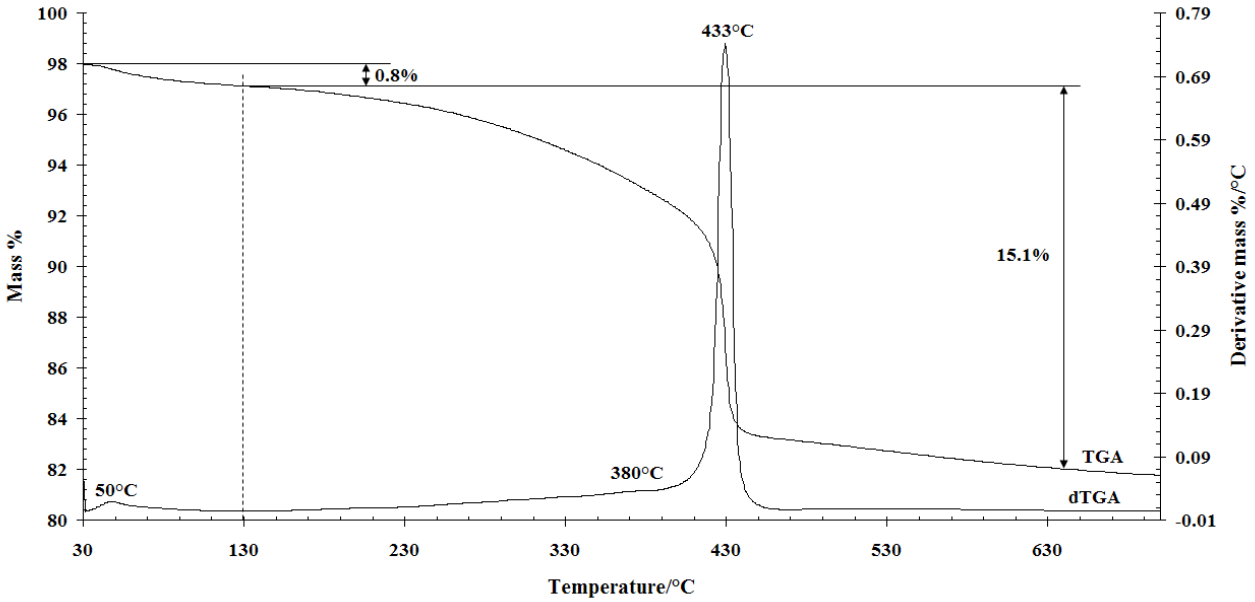

365

366

367 **Figure 4(c) 3 day 10% Cr-doped**

368

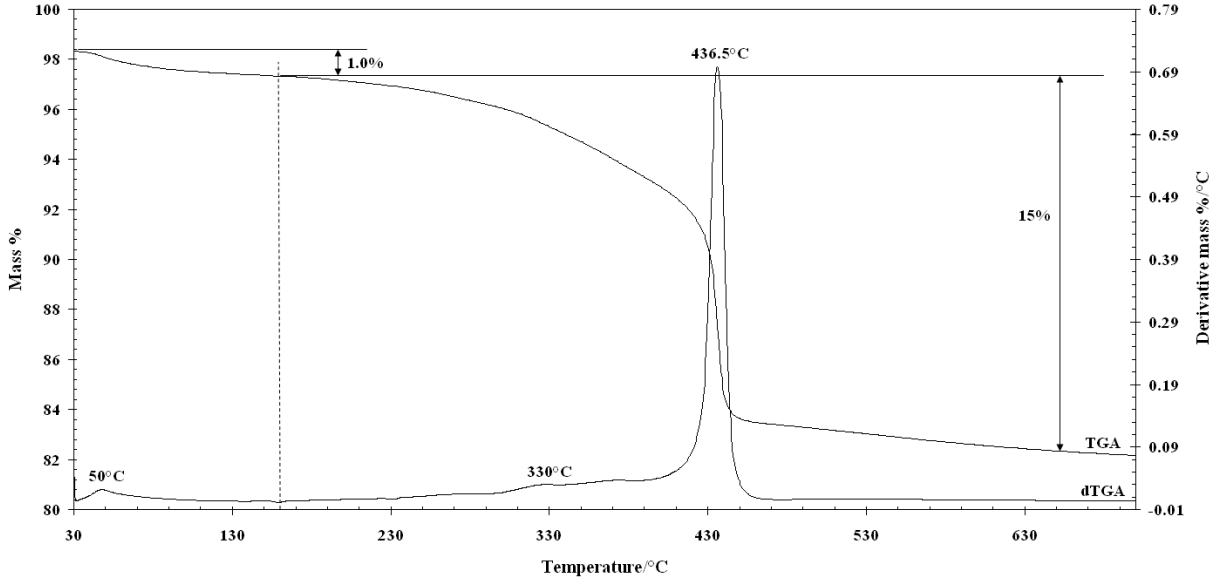

369

370

371

372 **Figure 4(d) 3 day 20% Cr-doped**

373

374

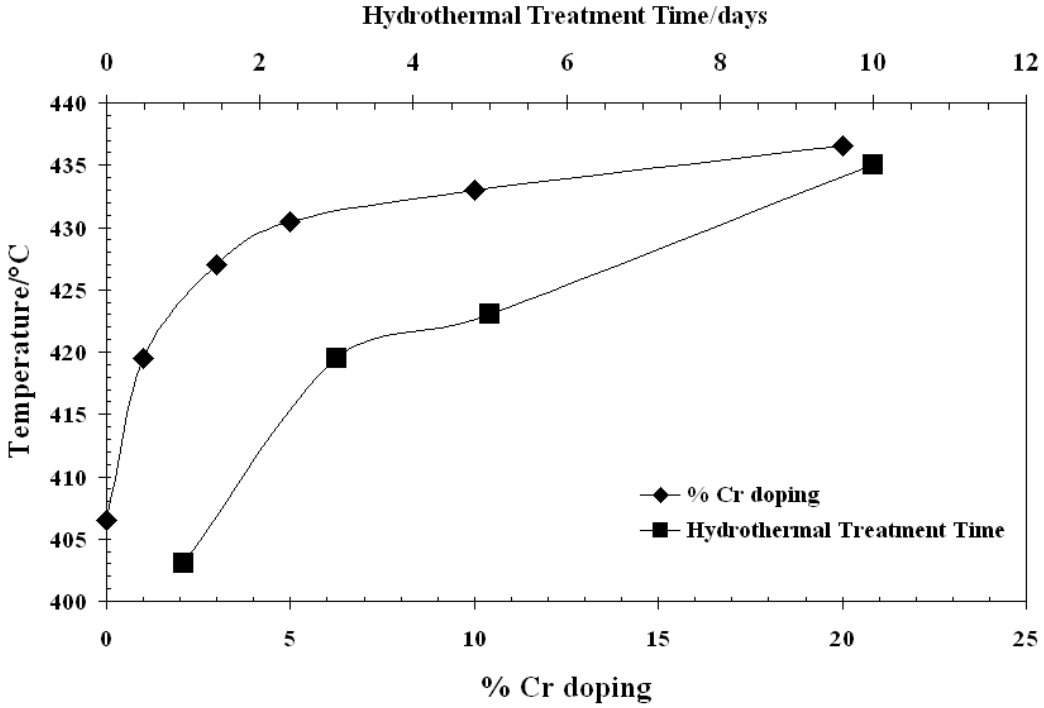

375

376

377 **Figure 5**

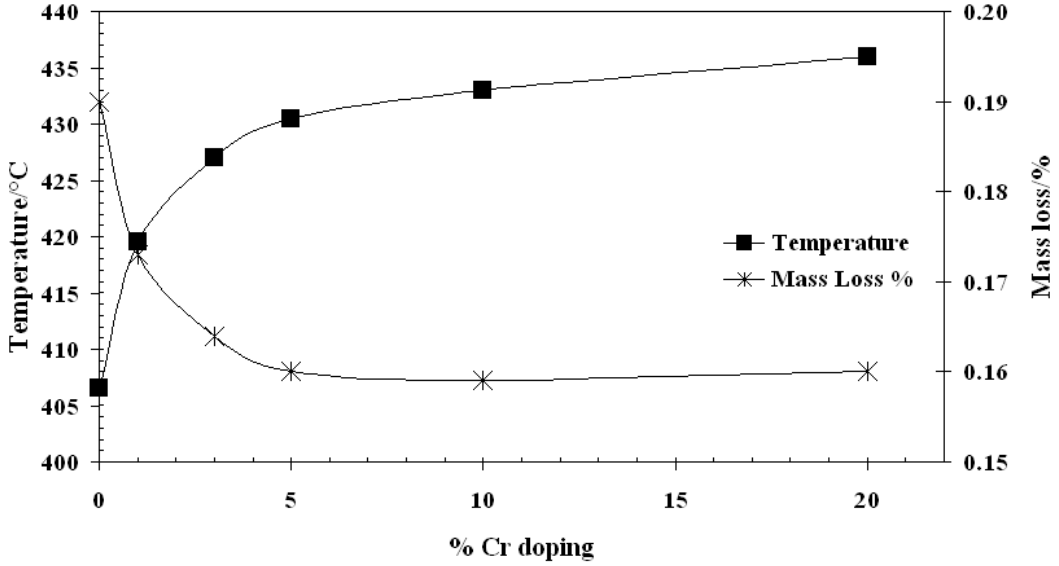
440
435
430
425
420
415
410
405
400
Temperature/°C
0.20
0.19
0.18
0.17
0.16
0.15
Mass loss/%
0
5
10
15
20
% Cr doping
Temperature
Mass Loss %

Figure 6

382

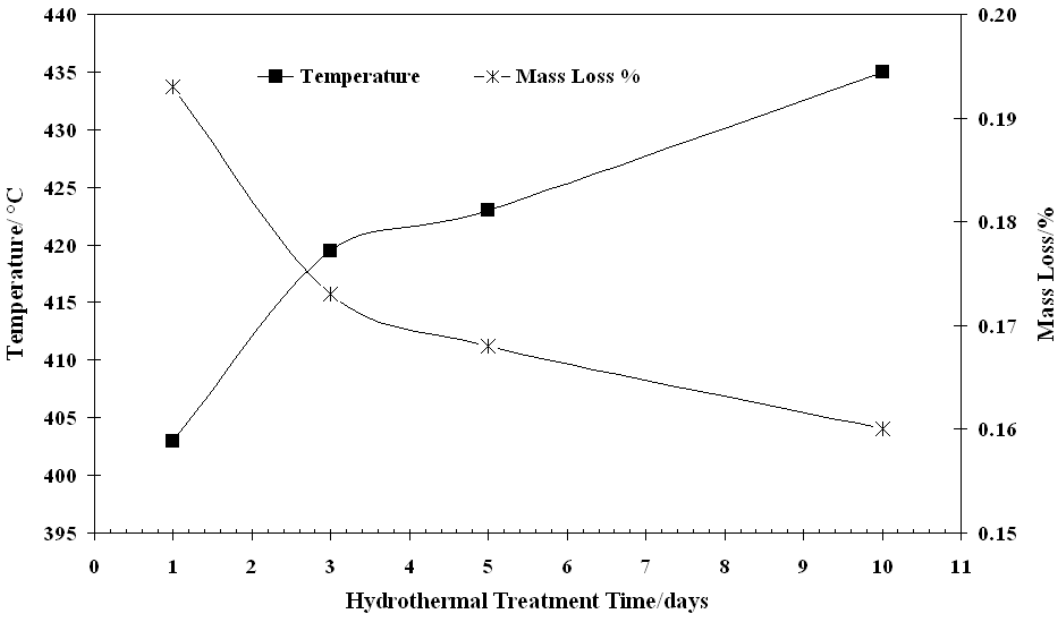

383

384

385

386 **Figure 7**